Building Damage Detection with UNet-Backbone Fusion in High-Resolution Satellite Imagery: 2023 Morocco Earthquake

Shimaa Holail[1], Tamer Saleh[2,3], Xiongwu Xiao[1,*], Amr H. Ali[2], Deren Li[1]

[1] State Key Laboratory of Information Engineering in Surveying, Mapping and Remote Sensing, Wuhan University, Wuhan 430072, China (shimaaholail; xwxiao; drli)@whu.edu.cn

[2] Geomatics Engineering Department, Faculty of Engineering at Shoubra, Benha University, Cairo 11629, Egypt (amrhali@feng.bu.edu.eg)

[3] School of Artificial Intelligence, Wuhan University, Wuhan, 430072, China (tamersaleh@whu.edu.cn)

KEY WORDS: Building Damage Detection, Morocco Earthquake, Satellite Imagery, xBD Dataset, UNet Model.

ABSTRACT:

Earthquakes and other natural disasters rank among the most destructive events, causing widespread loss of life and severe economic consequences globally. A primary consequence of earthquakes is the large-scale collapse and damage of buildings. The rapid advancement of high-resolution remote sensing technology, offering extensive coverage and multi-temporal capabilities, combined with deep learning methods, has opened new possibilities for accurately and efficiently detecting and assessing building damage to support crisis management. However, pre- and post-disaster images are often acquired under varying temporal, lighting, and weather conditions, complicating the task of accurately identifying building damage levels. This study proposes a Siamese network based on UNet to address these challenges, enabling the assessment of building damage using satellite imagery following earthquakes. The network leverages multi-scale feature differentiation to model spatial and temporal semantic relationships, addressing the issue of intra-class semantic variation. The proposed method was evaluated on the xBD disaster damage dataset and the 2023 Morocco earthquake dataset, achieving an overall accuracy of 95.5% and a kappa coefficient of 76.0%. These results highlight the potential of AI-driven solutions to meet the critical demands for speed and accuracy in disaster response scenarios.

1. INTRODUCTION

Natural disasters, such as earthquakes, rank among the most destructive phenomena, often causing significant loss of life, widespread infrastructure destruction, and severe economic setbacks (Hingorani et al., 2020; Perrone et al., 2020). The September 2023 Morocco earthquake highlighted these challenges, with entire communities experiencing extensive building collapses and damage (Oduoye et al., 2023). Accurately assessing the extent and severity of building damage is a critical component of disaster management, enabling the prioritization of rescue operations, resource allocation, and recovery planning (Krichen et al., 2024). Traditional damage assessment methods, such as on-site surveys, are valuable but often time-consuming, costly, and constrained by physical accessibility, particularly in large-scale disasters or remote areas (Contreras et al., 2021; Giardina et al., 2024). Therefore, efficient and accurate methods to extract information within a reasonable time frame are essential. Synthetic aperture radar (SAR) data, alongside optical satellite imagery, provides large-scale, timely, and detailed damage assessments for natural disasters (Brunner et al., 2010; Ferrentino et al., 2021; Serifoglu Yilmaz et al., 2023; Saleh et al., 2024a). While SAR data can capture information under all weather conditions and is suitable for real-time analysis, interpreting building damage scores remains a challenge (Ge et al., 2020). For example, Jung et al. (2017) investigated the damage caused by the Lake Fire in the San Bernardino National Forest, California, USA, in June 2015, using multi-temporal interferometric SAR data. Their proposed method formulated a coherent change model, assuming two simplified layers to interpret interferometric coherence with full polarization, calculate damage probability, compare natural variations, and identify damaged areas. Saleh et al. (2024b) examined the damage caused by floods resulting from heavy rainfall and tornadoes in the Iran region on January 13, 2020, using multi-temporal SAR data from the DAM-Net network, alongside large-scale flood inundation mapping and identification of damaged buildings. Li et al. (2019a) studied the damage from the 2009 L'Aquila earthquake in Italy using Envisat SAR images. By applying the principal components of an improved principal component analysis (PCA) method combined with multi-texture techniques, they achieved favorable results for building damage detection (BDD). Similarly, Kim et al. (2023) proposed a contextual change analysis method to map damaged buildings from the 2016 Kumamoto earthquake using Kompsat-5 dual-time SAR data. This approach utilized novel texture features and achieved improved results while maintaining low false alarm rates in agricultural areas.

Unlike SAR data, optical satellite images are easier to interpret and process, making them the preferred choice for damage detection (Wang et al., 2024; Gomroki et al., 2024; Seydi et al., 2023). Tong et al. (2012) proposed a method to detect building collapses from the Wenchuan earthquake using 3D geometric changes, particularly elevation differences, derived from IKONOS stereo image pairs. Li et al. (2022) developed an SSD model combined with a convolutional block attention mechanism (SSD_CBAM) to detect damaged buildings from post-event UAV images of the 2008 Wenchuan earthquake. Similarly, Li et al. (2019b) analyzed building damage caused by Hurricane Sandy in the Caribbean using post-event satellite images. Janalipour and Mohammadzadeh (2015) introduced an adaptive network-based fuzzy inference system (ANFIS) model to detect urban building damage after the Bam earthquake in Iran, integrating a pre-event vector map with post-event high-resolution

* Corresponding author

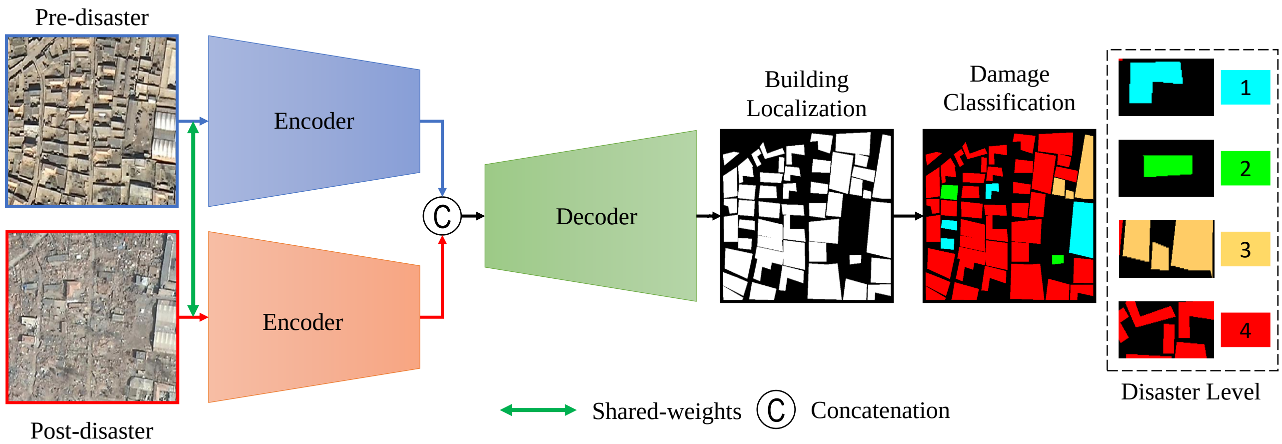

Figure 1. Overview of the proposed framework. Pre-processed pre- and post-disaster images are fed into the encoder and decoder, and building segmentation and damage classification masks are produced.

imagery. Holail et al. (2023) combined differential image features and attention modules using a learnable parameter along with deep supervision (DS) module to improve CNN performance and Hang et al. (2022) implemented a CNN-based segmentation network using high-resolution remote sensing data, while Ji et al. (2019) combined random forest (RF) and convolutional neural networks (CNN) to analyze satellite images from the 2010 Haiti earthquake, demonstrating superior performance of the CNN-RF combination. Xu et al. (2019) applied CNN-based machine learning for building damage detection across three disasters: the 2010 Haiti earthquake, the 2017 Mexico City earthquake, and the 2018 Indonesia earthquake. Other studies (Tilon et al., 2020; Zhao and Zhang, 2020; Shao et al., 2020; Shen et al., 2021; Da et al., 2022; Bai et al., 2020) utilized deep convolutional networks and transformers on xBD dataset satellite images to assess building damage before and after events. Lu et al. (2024) proposed a temporal binary attention transformer to identify building changes and damage by excluding irrelevant information in temporal remote sensing images, producing detailed damage maps. Holail et al. (2024) proposed a Siamese method that integrated an attention mechanism based on the temporal dimension of images to highlight subtle differences in damage levels, coupled with data augmentation strategies to mitigate class imbalance issues for detecting damaged buildings in a conflict zone.

Despite recent advancements, many approaches fail to account for the inherent ordering of ordinal damage labels, often simplifying building damage detection to a mere multi-class semantic segmentation task. For example, distinguishing between ”moderate” and ”severe” damage necessitates precise feature extraction, which is frequently obstructed by visual ambiguities such as debris, shadows, occlusions, or vegetation. Additionally, each disaster is inherently unique, even when similarities exist. For instance, building damage caused by one tornado may differ significantly from that caused by another. As a result, applying models trained on images from past disaster events to assess damage from new events requires rigorous evaluation on new datasets to assess the model’s adaptive performance. To address these challenges, this study introduces a UNet-based model designed to learn features at multiple scales and train a building damage detection network. The proposed method builds a hierarchy of multi-scale features to improve the localization and classification of changes between two input images. Several backbones are incorporated within the UNet framework as baselines for comparison. Furthermore, the model is trained on the xBD dataset to account for domain shifts across diverse disaster events. The effectiveness of the model is demonstrated through its application to the 2023 Morocco earthquake, utilizing 26 image pairs (512×512 pixels) with a high spatial resolution of 0.6 m/pixel. The primary contributions of this study are as follows:

1) A modified Siamese network based on UNet is proposed for building damage detection, leveraging multi-scale feature differentiation to effectively and efficiently model spatio-temporal semantic relationships between pre- and post-disaster images.

2) The proposed method’s effectiveness is evaluated using the 2023 Morocco earthquake dataset, providing a baseline for damage assessment tasks, demonstrating transfer learning capabilities, and assessing the model’s adaptive performance.

The remainder of the paper is organized as follows: Section 2 outlines the proposed method and evaluation metrics. Section 3 describes the dataset and presents experimental results. Finally, Section 4 concludes the study and discusses future research directions.

2. PROPOSED METHODOLOGY

2.1 Network Overview

Figure 1 presents an overview of the proposed multi-class change detection network for building damage assessment. The network is designed to perform two tasks simultaneously: building location identification and damage classification. It consists of a pair of pre- and post-disaster images, a Siamese U-Net-based encoder (E) that shares weights to learn hierarchical features, and a decoder (D) responsible for segmenting binary building masks and multi-class damage masks during the training stage. The encoder extracts features from the input images, while the decoder restores spatial dimensions and details through a deconvolution process. Initially, after preprocessing, which includes cropping, class imbalance optimization, and the application of data augmentation techniques, the images are fed into a pixel-level structure. In the encoder, a modified U-Net model (He et al., 2023) is used to generate a feature-based hierarchical difference block. The features from the i-th stage level $E_x(i)$, where $x \in \{\text{pre}, \text{post}\}$, are passed to the difference block Z, producing the common difference features z_i as output. These features represent the building polygons. Multiple backbones are employed for pre-training and performing binary semantic segmentation at the pixel level to predict whether each pixel belongs to a building. We tested VGG16, MobileNetV2, EfficientNet, and ResNet as backbones and classified the damage level of each building.

Specifically, the U-Net model is trained on the xBD dataset using pre- and post-disaster images, which serve as the pre-trained backbone for the damage assessment task. To capture the differences between pre- and post-disaster images, the features extracted from each clustering stage of the encoder are combined via concatenation. The decoder D is then used to reconstruct the output at the pixel level. The multi-scale features z_i, combined with the skip connections, are passed through the decoder D to achieve two-mask semantic segmentation of building locations. An upsampling operation is applied to the difference features, combined with previous features, to restore higher spatial dimensions, matching the size of the input images. The SoftMax function is applied to obtain the output of building locations, with values between (0, 1). For damage classification, the argmax function is applied to the final layer instead of SoftMax to obtain a five-class classification, where each pixel is assigned a value between 0 and 4. Here, 0 represents the background, and 1-4 correspond to buildings with damage levels ranging from no damage to completely destroyed. Finally, the Focal loss and Dice loss functions are applied during the training process for semantic segmentation. For the damage classification loss, we incorporate the multi-class cross-entropy loss, as formulated in (1).

$$
\begin{aligned}
L_{\text{Dice}} &= 1 - \frac{2P_t}{P+T} \\
L_{\text{Focal}} &= \begin{cases} -\alpha(1-P_t)^2 \log(P_t), & y = 1 \\ -(1-\alpha)(P_t)^2 \log(1-P_t), & y = 0 \end{cases} \\
L_{\text{cls}} &= -\frac{1}{N} y \log(p)
\end{aligned} \tag{1}
$$

where T represents the true value, P the predicted value, y the label value, P_t the number of positive samples, α the weighting factor, 0 indicating the absence of a building, 1 indicating the presence of a building, N the number of classes, p the class probability of the predicted sample, and y the one-hot encoded vector.

2.2 Encoder blocks

The U-Net encoder block follows the ResNet architecture, as illustrated in Fig. 2. It consists of a convolutional layer with a kernel size of 1×1, which serves to reduce the number of features. This is followed by a single convolutional layer with a kernel size of 3×3 to maintain the feature count. The final convolution also uses a 1×1 kernel. Both the first and second convolutional layers are followed by batch normalization (BNorm) and ReLU activation functions. Additionally, the output of the final convolution is processed by a squeeze-and-excite module (SEM) that adaptively recalibrates the importance of each channel's features (Hu et al., 2018). The output is then added back to the block's input through a residual connection. If there is a mismatch in the number of input and output features, an additional pointwise convolution with batch normalization is applied along the residual path to align the output shape, enabling element-wise summation. This result is then passed through another ReLU activation.

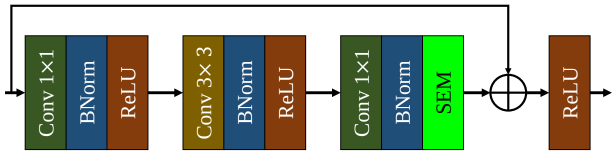

Figure 2. Convolutional blocks used in U-Net encoder with squeeze-and-excite module.

2.3 Evaluation metrics

Four metrics were utilized to validate the accuracy and effectiveness of the proposed method in comparing the ground truth and predicted change map. These metrics include Overall Accuracy (OA), Precision (P), Recall (R), and F1-score. The formulas for these metrics are provided below:

$$
\begin{aligned}
\text{OA} &= \frac{TP+TN}{TP+FN+TN+FP} \\
\text{Precision} &= \frac{TP}{TP+FP} \\
\text{Recall} &= \frac{TP}{TP+FN} \\
F_{\text{loc}} &= \frac{\text{2TP}}{\text{2TP + FP+ FN}} \\
F_{\text{cls}} &= \frac{4}{\sum_{i=1}^{4} \frac{1}{F_{1_{Ci}}}} \\
F_1^{\text{all}} &= \alpha \cdot F_{\text{loc}} + \beta \cdot F_{\text{cls}}
\end{aligned} \tag{2}
$$

where TP = total number of true positives for all classes
FN = false negatives
FP = false positives
TN = true negatives

3. EXPERIMENTAL RESULTS

3.1 Materials and Dataset

3.1.1 xBD Dataset: The xBD dataset is a large-scale collection of building samples from seven disaster types across 19 natural disaster events, obtained from multiple satellite platforms, including WorldView-2 and WorldView-3, and serves as a benchmark for building damage assessment Gupta et al. (2019). It comprises 11,034 pairs of high-resolution optical satellite images, covering a total area of 45,361.79 sq-km and including 850,736 building polygons. Each image pair consists of a pre-disaster and a post-disaster image. The dataset categorizes damage into four levels: no damage, minor damage, major damage, and devastating damage. In this study, the xBD dataset was utilized, with 70% of the data allocated for training and 30% for validation to evaluate building damage levels effectively.

3.1.2 Morocco Earthquake 2023:

Morocco is situated on the northwestern edge of the African Plate, which is in continuous convergence and collision with the Eurasian Plate. On September 8, 2023, a 6.8-magnitude earthquake struck the High Atlas Mountains, 71 km southwest of Marrakesh, marking one of the most violent earthquakes in Morocco's history. The epicenter was located at 31.058°N and 8.490°W, with a focal depth of 26 km according to the Euro-Mediterranean Seismological Center and 27.8 km as reported by the Global Centroid Moment Tensor (CMT) project Ziraoui et al. (2024); Touati et al. (2024). According to the Moroccan Ministry of Interior, at least 2,901 people were killed, primarily in Marrakesh and five governorates near the epicenter, while approximately 320,000 people were affected. Remote villages in the High Atlas Mountains suffered severe losses and extensive structural damage. The earthquake's impact was intensified by the vulnerability of the building stock and its occurrence at night when most people were at home Cheloni et al. (2024); Yeck et al. (2023). Figure 3

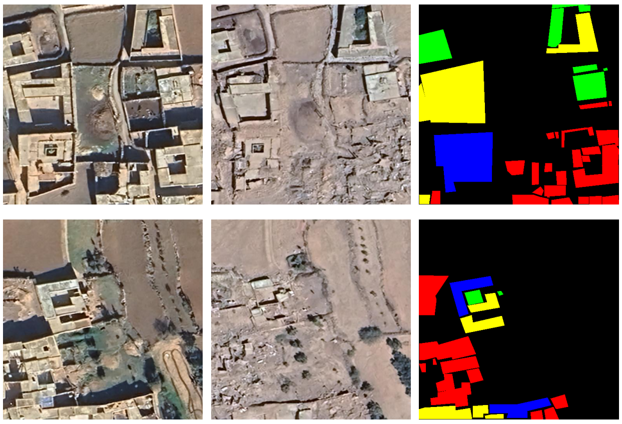

(a) (b) (c)

Figure 3. Sample from Morocco earthquake dataset. (a) Image acquired in Dec 2022 as a pre-event reference. (b) Image taken on September 9, 2023, after the Morocco earthquake. (c) The ground truth.

presents a WorldView-II image of Marrakesh and the corresponding ground truth, highlighting the city's dense urban layout and significant post-earthquake damage. Polygons representing damaged and undamaged buildings were plotted in QGIS and layered with unique identifiers to generate the ground truth. Following training on the xBD dataset, the Morocco earthquake dataset was employed for prediction purposes.

3.2 Implementation details

The experiments were conducted using the PyTorch framework [1] on an NVIDIA GRID RTX8000-8Q GPU with 8 GB memory to ensure optimal performance. The network optimization utilized the AdamW optimizer and a one-cycle learning rate policy, with an initial learning rate of 0.0001, momentum of 0.9, and a weight decay of 0.0002. To address the limited size of the Morocco earthquake dataset, data augmentation techniques, including random flipping, rotation, and random cropping, were applied to the input image patches during training. The batch size was set to two, and the input image size was fixed at 512 × 512 pixels. The models were trained for 100 epochs, with weights saved every 20 epochs. The model achieving the highest F1 score was selected for inference across various test locations.

[1] https://pytorch.org

Model	Accuracy	Precision	Recall	Kappa
VGG16	0.942	0.742	0.486	0.653
MobileNetV2	0.942	0.727	0.482	0.654
EfficientNet	0.948	0.592	0.490	0.737
ResNet50	0.953	0.724	0.537	0.746
ResNet18	0.952	0.639	0.514	0.752
ResNet34	0.955	0.704	0.545	0.760

Table 1. Quantitative evaluation of results on the xBD dataset.

3.3 Results and analysis

To evaluate the performance of the proposed method outlined in Section 2.1, we assessed its segmentation capabilities using several accuracy evaluation metrics to compare model performance. The backbone architectures employed in this study included VGG-16, EfficientNet, MobileNetV2, ResNet18, ResNet50, and ResNet34. Table 1 presents the comparative results of these models on the xBD training dataset. Among them, the ResNet34 backbone demonstrated superior performance in the building localization task across multiple evaluation metrics, achieving a K-score of 76.0% and an overall accuracy of 95.5%. Notably, the K-score showed a 10.7% improvement over the VGG-16 model. Figure 4 illustrates the prediction results on the xBD test set. Comparing the result maps of various models, the ResNet34 model demonstrates significantly higher accuracy and effectively reduces false positives compared to other models. Additionally, it provides a more complete classification of buildings, closely aligning with the ground truth, and better distinguishes building damage levels. In contrast, the VGG16 model exhibits numerous missed detections and false positives, reducing accuracy.

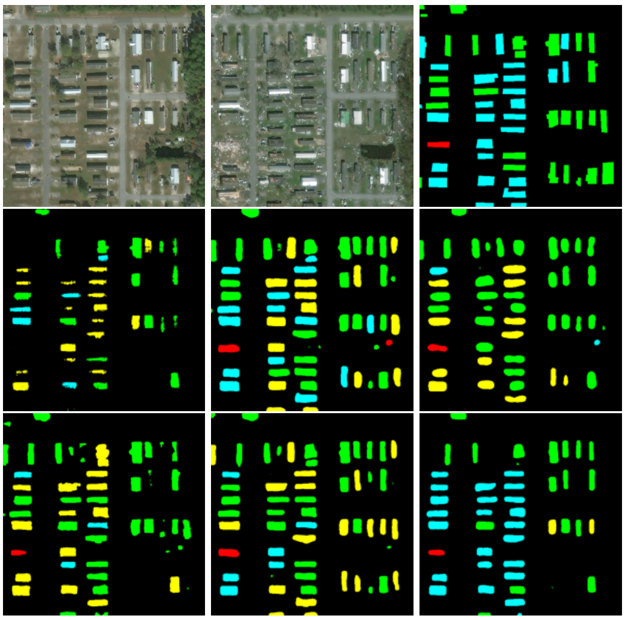

Figure 4. Visual comparison of different models on a test sample from the xBD dataset: Pre-disaster image, post-disaster image, ground truth, VGG16, EfficientNet, MobileNetV2, ResNet18, ResNet50, and ResNet34 (in order).

Additionally, Table 2 reports the evaluation metrics for damage classification, integrating the building localization results on the

Backbone	F_1^{all}	F_1^{loc}	F_1^{damg}	Damage F_1 score per class			
				Intact	Minor	Major	Destroyed
EfficientNet (Tan and Le, 2019)	60.5	82.9	50.9	77.5	42.4	19.2	64.5
MobileNetV2 (Sandler et al., 2018)	61.9	73.5	57.0	66.1	39.9	52.9	69.1
VGG16 (Abouelyazid, 2022)	62.3	73.1	57.6	65.8	40.8	54.4	69.6
ResNet18 (He et al., 2016)	63.7	83.6	55.2	78.3	42.6	33.2	66.8
ResNet50 (He et al., 2016)	67.2	82.1	60.8	77.2	40.7	52.1	73.1
ResNet34 (He et al., 2016)	67.7	83.7	60.8	78.4	43.7	48.6	72.4

Table 2. Quantitative comparison of different backbone models on the 2023 Morocco earthquake dataset (%).

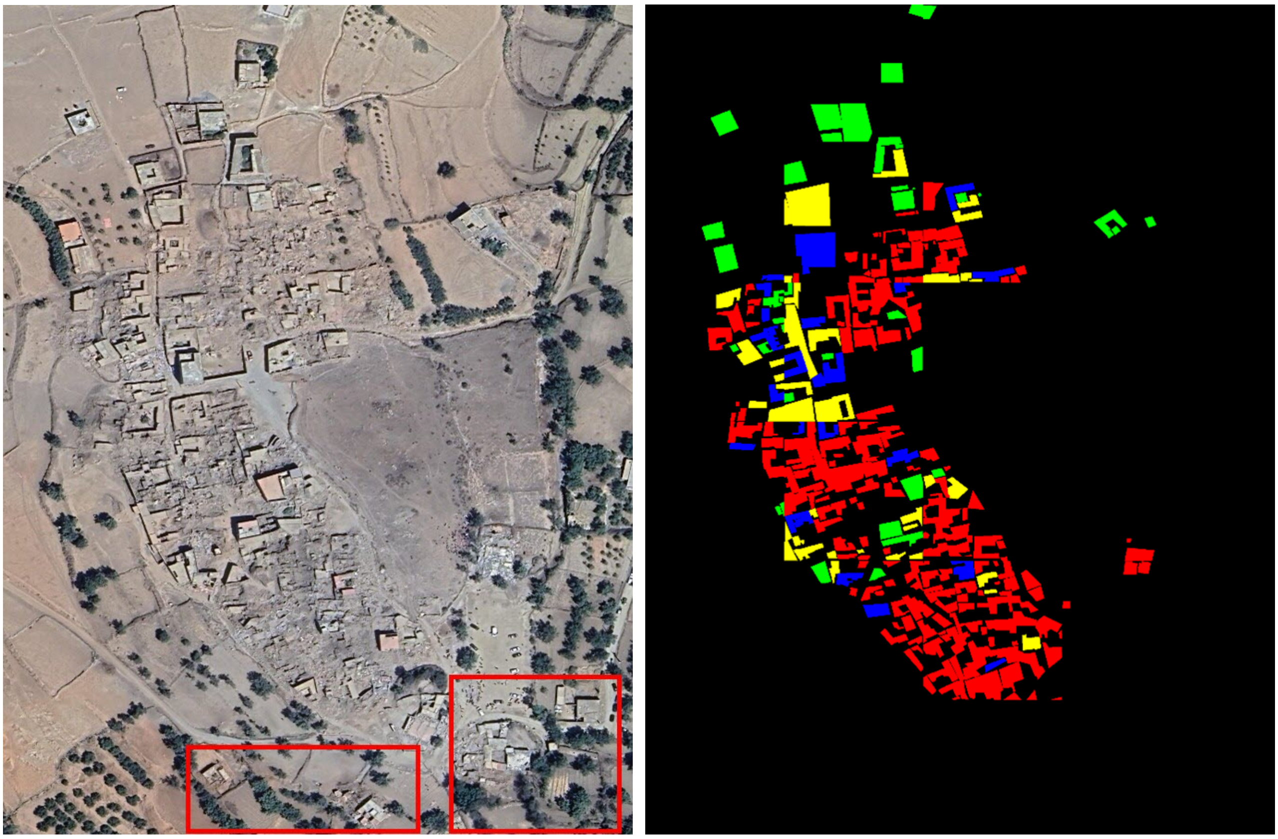

(a) (b)

Figure 5. Results of the proposed method on the Morocco earthquake dataset: (a) Post-disaster image (Sept 9, 2023), (b) Output of the proposed method.

Morocco earthquake dataset. The ResNet34 model achieved an overall F1 score of 67.7%, with F_{loc} and F_{damg} scores of 83.7% and 60.8%, respectively. The F1 scores for the damage classes: intact, minor damage, major damage, and destruction were 78.4%, 43.7%, 48.6%, and 72.4%, respectively. Compared to EfficientNet, ResNet34 exhibited a significant improvement in accuracy, with an overall F_{overall} increase of 7.2%. These results demonstrate that the proposed network model, utilizing ResNet34 as its backbone, achieves high accuracy in identifying building damage levels across various damage categories. Figure 5 presents the results of the 2023 Morocco earthquake test using the proposed network, trained on the xBD dataset. The network effectively distinguishes damage levels of buildings and reconstructs their boundaries. However, as highlighted by the red box in Figure 5(a), further improvements are needed to detect certain damaged buildings that the current model failed to identify.

4. CONCLUSIONS

This paper presents a Siamese model for identifying and assessing building damage severity, utilizing U-Net and ResNet34 as the backbone. The model leverages the weight-sharing capability of the Siamese network to extract and compare features from pre- and post-disaster building images. Integrating an encoder-decoder structure enhances feature extraction and captures richer image semantic information. The model's performance was evaluated on the xBD dataset and the untrained 2023 Morocco earthquake dataset for damage classification tasks. Experimental results demonstrate that the proposed model achieves superior performance across various evaluation metrics in building damage detection, showcasing its potential for cross-disaster damage assessment. This capability can provide a deep learning-based solution for timely disaster response and humanitarian assistance during emergencies. However, this study has limitations. Generating diverse levels of earthquake-damaged building data remains challenging. While the xBD dataset was used for training, it does not accurately represent real-world scenarios due to its limited earthquake data, covering only a single event. Future work will focus on incorporating datasets from diverse disaster scenarios, such as wars, forest fires, and additional earthquake events, to further validate the model's effectiveness. Additionally, efforts will be made to improve the efficiency of annotating varying degrees of building damage for the Morocco earthquake dataset and other disaster types, addressing the scarcity of similar disaster data and meeting the urgent needs of disaster response.

ACKNOWLEDGMENT

This work was supported by the Natural Science Foundation of Hubei Province (Grant No. 2022CFB773), the National Natural Science Foundation of China (Grant No. 42101449), the National Key Research and Development Program of China (Grant No. 2023YFB3906102), and the Chutian Scholar Program of Hubei Province.

References

Abouelyazid, M., 2022. Comparative Evaluation of VGG-16 and U-Net Architectures for Road Segmentation. *Eigenpub Review of Science and Technology*, 6(1), 75–91.

Bai, Y., Hu, J., Su, J., Liu, X., Liu, H., He, X., Meng, S., Mas, E., Koshimura, S., 2020. Pyramid pooling module-based semi-siamese network: A benchmark model for assessing building damage from xBD satellite imagery datasets. *Remote Sensing*, 12(24), 4055.

Brunner, D., Lemoine, G., Bruzzone, L., 2010. Earthquake damage assessment of buildings using VHR optical and SAR imagery. *IEEE Transactions on Geoscience and Remote Sensing*, 48(5), 2403–2420.

Cheloni, D., Famiglietti, N. A., Tolomei, C., Caputo, R., Vicari, A., 2024. The 8 September 2023, MW 6.8, Morocco earthquake: A deep transpressive faulting along the active high Atlas mountain belt. *Geophysical Research Letters*, 51(2), e2023GL106992.

Contreras, D., Wilkinson, S., James, P., 2021. Earthquake reconnaissance data sources, a literature review. *Earth*, 2(4), 1006–1037.

Da, Y., Ji, Z., Zhou, Y., 2022. Building damage assessment based on siamese hierarchical transformer framework. *Mathematics*, 10(11), 1898.

Ferrentino, E., Nunziata, F., Bignami, C., Graziani, L., Maramai, A., Migliaccio, M., 2021. Multi-polarization C-band SAR imagery to quantify damage levels due to the Central Italy earthquake. *International Journal of Remote Sensing*, 42(15), 5969–5984.

Ge, P., Gokon, H., Meguro, K., 2020. A review on synthetic aperture radar-based building damage assessment in disasters. *Remote Sensing of Environment*, 240, 111693.

Giardina, G., Macchiarulo, V., Foroughnia, F., Jones, J. N., Whitworth, M. R., Voelker, B., Milillo, P., Penney, C., Adams, K., Kijewski-Correa, T., 2024. Combining remote sensing techniques and field surveys for post-earthquake reconnaissance missions. *Bulletin of Earthquake Engineering*, 22(7), 3415–3439.

Gomroki, M., Hasanlou, M., Chanussot, J., Hong, D., 2024. EMYNET-BDD: efficientvitb meets YOLOV8 in the encoder-decoder architecture for building damage detection using post-event remote sensing images. *IEEE Journal of Selected Topics in Applied Earth Observations and Remote Sensing*.

Gupta, R., Goodman, B., Patel, N., Hosfelt, R., Sajeev, S., Heim, E., Doshi, J., Lucas, K., Choset, H., Gaston, M., 2019. Creating xbd: A dataset for assessing building damage from satellite imagery. *Proceedings of the IEEE/CVF conference on computer vision and pattern recognition workshops*, 10–17.

Hang, R., Yang, P., Zhou, F., Liu, Q., 2022. Multiscale progressive segmentation network for high-resolution remote sensing imagery. *IEEE Transactions on Geoscience and Remote Sensing*, 60, 1–12.

He, K., Zhang, X., Ren, S., Sun, J., 2016. Deep residual learning for image recognition. *Proceedings of the IEEE Conference on Computer Vision and Pattern Recognition (CVPR)*.

He, Y., Wang, J., Liao, C., Zhou, X., Shan, B., 2023. MS4D-Net: Multitask-Based Semi-Supervised Semantic Segmentation Framework with Perturbed Dual Mean Teachers for Building Damage Assessment from High-Resolution Remote Sensing Imagery. *Remote Sensing*, 15(2), 478.

Hingorani, R., Tanner, P., Prieto, M., Lara, C., 2020. Consequence classes and associated models for predicting loss of life in collapse of building structures. *Structural Safety*, 85, 101910.

Holail, S., Saleh, T., Xiao, X., Li, D., 2023. Afde-net: Building change detection using attention-based feature differential enhancement for satellite imagery. *IEEE Geoscience and Remote Sensing Letters*, 20, 1–5.

Holail, S., Saleh, T., Xiao, X., Xiao, J., Xia, G.-S., Shao, Z., Wang, M., Gong, J., Li, D., 2024. Time-series satellite remote sensing reveals gradually increasing war damage in the Gaza Strip. *National Science Review*, 11(9), nwae304.

Hu, J., Shen, L., Sun, G., 2018. Squeeze-and-excitation networks. *Proceedings of the IEEE conference on computer vision and pattern recognition*, 7132–7141.

Janalipour, M., Mohammadzadeh, A., 2015. Building damage detection using object-based image analysis and ANFIS from high-resolution image (case study: BAM earthquake, Iran). *IEEE Journal of Selected Topics in Applied Earth Observations and Remote Sensing*, 9(5), 1937–1945.

Ji, M., Liu, L., Du, R., Buchroithner, M. F., 2019. A comparative study of texture and convolutional neural network features for detecting collapsed buildings after earthquakes using pre-and post-event satellite imagery. *Remote Sensing*, 11(10), 1202.

Jung, J., Kim, D.-j., Yun, S.-h., Lavalle, M., 2017. Damage mapping based on coherence model using multi-temporal polarimetric-interferometric uavsar data. *2017 IEEE International Geoscience and Remote Sensing Symposium (IGARSS)*, IEEE, 189–192.

Kim, M., Park, S.-E., Lee, S.-J., 2023. Detection of damaged buildings using temporal SAR data with different observation modes. *Remote Sensing*, 15(2), 308.

Krichen, M., Abdalzaher, M. S., Elwekeil, M., Fouda, M. M., 2024. Managing natural disasters: An analysis of technological advancements, opportunities, and challenges. *Internet of Things and Cyber-Physical Systems*, 4, 99–109.

Li, Q., Gong, L., Zhang, J., 2019a. A correlation change detection method integrating PCA and multi-texture features of SAR image for building damage detection. *European Journal of Remote Sensing*, 52(1), 435–447.

Li, X., Yang, J., Li, Z., Yang, F., Chen, Y., Ren, J., Duan, Y., 2022. Building damage detection for extreme earthquake disaster area location from post-event uav images using improved ssd. *IGARSS 2022-2022 IEEE International Geoscience and Remote Sensing Symposium*, IEEE, 2674–2677.

Li, Y., Hu, W., Dong, H., Zhang, X., 2019b. Building damage detection from post-event aerial imagery using single shot multibox detector. *Applied Sciences*, 9(6), 1128.

Lu, W., Wei, L., Nguyen, M., 2024. Bi-temporal attention transformer for building change detection and building damage assessment. *IEEE Journal of Selected Topics in Applied Earth Observations and Remote Sensing*.

Oduoye, M. O., Rehman, L. U., Ubechu, S. C., Abdulkareem, L., Mourid, M. R., Irfan, H., 2023. Urgent call to action: Supporting Morocco in the aftermath of the recent earthquake. *Journal of Global Health*, 13.

Perrone, D., O’Reilly, G. J., Monteiro, R., Filiatrault, A., 2020. Assessing seismic risk in typical Italian school buildings: From in-situ survey to loss estimation. *International journal of disaster risk reduction*, 44, 101448.

Saleh, T., Holail, S., Xiao, X., Xia, G.-S., 2024a. High-precision flood detection and mapping via multi-temporal SAR change analysis with semantic token-based transformer. *International Journal of Applied Earth Observation and Geoinformation*, 131, 103991.

Saleh, T., Weng, X., Holail, S., Hao, C., Xia, G.-S., 2024b. DAM-Net: Flood detection from SAR imagery using differential attention metric-based vision transformers. *ISPRS Journal of Photogrammetry and Remote Sensing*, 212, 440–453.

Sandler, M., Howard, A., Zhu, M., Zhmoginov, A., Chen, L.-C., 2018. Mobilenetv2: Inverted residuals and linear bottlenecks. *Proceedings of the IEEE Conference on Computer Vision and Pattern Recognition (CVPR)*.

Serifoglu Yilmaz, C., Yilmaz, V., Tansey, K., Aljehani, N. S., 2023. Automated detection of damaged buildings in post-disaster scenarios: a case study of Kahramanmaraş (Türkiye) earthquakes on February 6, 2023. *Natural Hazards*, 119(3), 1247–1271.

Seydi, S. T., Hasanlou, M., Chanussot, J., Ghamisi, P., 2023. BDD-Net+: A building damage detection framework based on modified coat-net. *IEEE Journal of Selected Topics in Applied Earth Observations and Remote Sensing*, 16, 4232–4247.

Shao, J., Tang, L., Liu, M., Shao, G., Sun, L., Qiu, Q., 2020. BDD-Net: A general protocol for mapping buildings damaged by a wide range of disasters based on satellite imagery. *Remote sensing*, 12(10), 1670.

Shen, Y., Zhu, S., Yang, T., Chen, C., Pan, D., Chen, J., Xiao, L., Du, Q., 2021. Bdanet: Multiscale convolutional neural network with cross-directional attention for building damage assessment from satellite images. *IEEE Transactions on Geoscience and Remote Sensing*, 60, 1–14.

Tan, M., Le, Q., 2019. EfficientNet: Rethinking model scaling for convolutional neural networks. K. Chaudhuri, R. Salakhutdinov (eds), *Proceedings of the 36th International Conference on Machine Learning*, Proceedings of Machine Learning Research, 97, PMLR, 6105–6114.

Tilon, S., Nex, F., Kerle, N., Vosselman, G., 2020. Post-disaster building damage detection from earth observation imagery using unsupervised and transferable anomaly detecting generative adversarial networks. *Remote sensing*, 12(24), 4193.

Tong, X., Hong, Z., Liu, S., Zhang, X., Xie, H., Li, Z., Yang, S., Wang, W., Bao, F., 2012. Building-damage detection using pre-and post-seismic high-resolution satellite stereo imagery: A case study of the May 2008 Wenchuan earthquake. *ISPRS Journal of Photogrammetry and Remote Sensing*, 68, 13–27.

Touati, B., Gu, W., Ni, S., Chu, R., Sheng, M., Xue, Q., Bellalem, F., Maouche, S., Yahyaoui, H., 2024. The 2023 M w 6.8 Adassil Earthquake (Chichaoua, Morocco) on a steep reverse fault in the deep crust and its geodynamic implications. *Earth and Planetary Physics*, 8(3), 522–534.

Wang, L., Wu, J., Yang, Y., Tang, R., Ya, R., 2024. Deep Learning Models for Hazard-Damaged Building Detection Using Remote Sensing Datasets: A Comprehensive Review. *IEEE Journal of Selected Topics in Applied Earth Observations and Remote Sensing*.

Xu, J. Z., Lu, W., Li, Z., Khaitan, P., Zaytseva, V., 2019. Building damage detection in satellite imagery using convolutional neural networks. *arXiv preprint arXiv:1910.06444*.

Yeck, W. L., Hatem, A. E., Goldberg, D. E., Barnhart, W. D., Jobe, J. A. T., Shelly, D. R., Villaseñor, A., Benz, H. M., Earle, P. S., 2023. Rapid Source Characterization of the 2023 M w 6.8 Al Haouz, Morocco, Earthquake. *The Seismic Record*, 3(4), 357–366.

Zhao, F., Zhang, C., 2020. Building damage evaluation from satellite imagery using deep learning. *2020 IEEE 21st International Conference on Information Reuse and Integration for Data Science (IRI)*, IEEE, 82–89.

Ziraoui, A., Kissi, B., Aaya, H., Mrabet, N., Azdine, I., 2024. Seismic risk assessment, damage estimation, and strengthening of seismic construction standards in Morocco. *Journal of Building Pathology and Rehabilitation*, 9(1), 79.